



Liu, R., Phillips, D.B., Li, F., Williams, M.D., Andrews, D.L., and Padgett, M.J. (2015) Discrete emitters as a source of orbital angular momentum. *Journal of Optics*, 17(4), 045608.

Copyright © 2015 IOP Publishing

A copy can be downloaded for personal non-commercial research or study, without prior permission or charge

Content must not be changed in any way or reproduced in any format or medium without the formal permission of the copyright holder(s)

<http://eprints.gla.ac.uk/104665/>

Deposited on: 07 April 7, 2015

Enlighten – Research publications by members of the University of Glasgow
<http://eprints.gla.ac.uk>

Discrete emitters as a source of orbital angular momentum

R. Liu,^{1,2} D. B. Phillips,^{1,*} F. Li,² M. D. Williams,³ D. L. Andrews,³ and M. J. Padgett¹

¹*SUPA, School of Physics and Astronomy, University of Glasgow, Glasgow, G12 8QQ, UK.*

²*Department of Applied Physics, School of Science, Xi'an Jiaotong University, People's Republic of China.*

³*School of Chemistry, University of East Anglia, Norwich Research Park, Norwich NR4 7TJ, UK.*

Generation of light carrying orbital angular momentum (OAM) is of fundamental interest due to its applications in a broad range of fields, such as classical and quantum optical communications, and optical micro-manipulation. Light carrying a well defined state of OAM is typically created by imparting an azimuthally varying phase structure onto a plane wave. In this work, we investigate, using numerical simulations and experiments, the OAM spectra of light radiated from a heavily course grained emission pattern: an array of discrete circular apertures arranged in a ring configuration, with a constant phase increment between adjacent apertures. We show how the number of apertures and their relative phase defines the position and spacing of peaks in the OAM spectra. We demonstrate that by spatially filtering beams emitted from such a configuration, higher order peaks in the OAM spectra can be suppressed, leaving a single dominant lowest order peak, and recovering a beam carrying a well-defined OAM state. We qualitatively interpret the efficiency of generating beams this way in terms of the angular uncertainty principle.

A light beam carrying a defined state of orbital angular momentum (OAM) has a complex field characterised by $e^{i\ell\theta}$, where θ is the azimuthal angle about the optical axis, and ℓ is the topological charge. Mode number ℓ describes how many integer multiples of 2π the phase changes by around one circuit of the vortex core. The helical phase gradient results in a Poynting vector that is azimuthally skewed with respect to the optical axis, and therefore such beams can be used to exert torque on micro-scale objects [1, 2], and measure rotation rate of remote spinning bodies [3, 4]. Higher values of $|\ell|$ define more highly twisted wavefronts, and as ℓ is a theoretically unbounded degree of freedom there has also been much investigation into the use of light beams carrying OAM for generating a multi-state alphabet for classical and quantum optical communications [5–7].

Beams carrying OAM have been generated in a variety of ways: at first by transforming a Hermite-Gaussian to Laguerre-Gaussian beam using cylindrical lenses [8], and also by binary amplitude modulation using a spiral zone plate to encode an azimuthally varying phase structure onto a plane wavefront [9, 10]. Most commonly, spatial light modulators (SLMs) that act as spatially programmable diffractive elements are used: by combining the required azimuthally varying phase pattern with a phase tilt to produce a forked grating hologram, light carrying the desired mode of OAM is transmitted into the first order of the diffraction pattern with high efficiency [11, 12]. Recently the generation of vortex beams using micro-scale silicon integrated photonic devices has been demonstrated [13, 14], and it has also been theoretically shown that beams carrying OAM can be produced

by a chiral annulus of oriented dipole-emitters, where the phase relationship between them is defined by the wavefunction of the whole system [15, 16].

All of these methods rely on imparting a spatially dependent phase onto the emitted field to generate the desired state. Recently there has been increasing interest in simplified methods to generate beams carrying OAM, specifically for non-optical regimes where the equivalent to spatial light modulator technology does not currently exist [17–21]. This often requires the fabrication of one-off masks, and simplification of mask designs can potentially facilitate such techniques.

In this work we aim to investigate, through a combination of experiments and scalar wave optics simulations, how light beams carrying defined states of OAM can be generated from simplified phase patterns: a set of a few discrete apertures of fixed relative phase. The circular apertures are equally spaced in a ring configuration, with a constant relative phase step between adjacent apertures. We measure the OAM spectrum of our emitted beams and show how this depends upon the relative size of the apertures and the ring, show how spatial filtering can be used to purify the output to produce a well defined OAM state, and consider the efficiency of the beam generation in terms of the angular uncertainty principle.

MODAL DECOMPOSITION

An optical field $U(r, \theta)$ (where r and θ define the radius and azimuthal angle respectively in a cylindrical coordinate system) can be described as a linear superposition of orthogonal complex valued modes Ψ_i of a particular

*Electronic address: david.phillips@glasgow.ac.uk

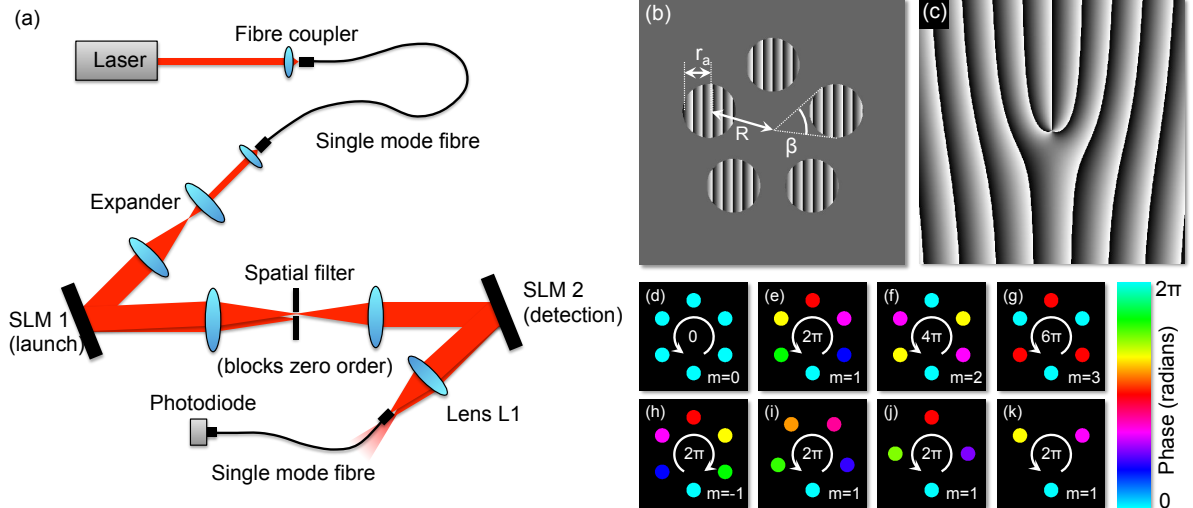


FIG. 1: (a) Schematic of experimental set up. The diagram shows how the spatial filter is used to block undesired diffraction orders from SLM 1. Only light flattened to a plane wave is focussed into the fibre coupler after SLM 2. (b) An example of the phase hologram displayed by SLM 1. (c) An example of the phase hologram at SLM 2, used to measure the OAM spectrum of the beam. $\ell = +2$ is shown in this case. In (b) and (c), the grey-scale level is mapped linearly to phase, with white = 0 and black = 2π . (d-k) A range of emitter phase patterns, for different values of n (the number of apertures) and m (the total integer multiple of 2π the phase changes by around the entire ring). The value given in the middle of each pattern is equal to $2\pi m$.

basis set:

$$U(r, \theta) = \sum_{i=1}^{\infty} c_i \Psi_i(r, \theta) \quad (1)$$

Here i indexes each orthogonal mode, and c_i are a set of complex coefficients defining the amplitude and relative phase of each mode. Coefficients c_i can be found by performing a modal decomposition, which exploits the orthonormal property of each mode:

$$\langle \Psi_i | \Psi_j \rangle = \iint \Psi_i^* \Psi_j r dr d\theta = \delta_{ij} \quad (2)$$

This states that the overlap integral between modes (also known as an inner product) is only non-zero for two modes of identical mode index. Therefore, the coefficients c_i describing the optical field $U(r, \theta)$ in the Ψ basis, may be found by taking the inner product of $U(r, \theta)$ with each mode in turn [22]:

$$c_i = \langle \Psi_i | U \rangle \quad (3)$$

In this work it is convenient to consider the Laguerre-Gaussian (LG) basis, as this orthogonal set of modes are stable upon propagation and each has a well defined OAM state described by ℓ [8, 23]. At a plane perpendicular to the optical axis, each LG mode is described by a 2D complex function, characterised by the azimuthal index ℓ , radial index p , and beam waist ω . In the formalism described above, each unique mode $LG_{\ell,p}$ is therefore assigned a unique index i .

The OAM spectrum describes the intensity of each mode ℓ , P_ℓ , summing over contributions from all values of radial index p that are representable with our experimental beam of finite area, therefore from $p=0$ to $p=p_{max}$:

$$P_\ell = \sum_{p=0}^{p_{max}} |c_{\ell,p}|^2 \quad (4)$$

As can be seen from the fact that we take the modulus square of $c_{\ell,p}$ in equation 4, the OAM spectrum contains no information about the relative phase of the modes, and therefore is invariant upon propagation of the beam, and so can be measured in any plane of the freely propagating beam.

To investigate the OAM spectrum of our simplified emission patterns theoretically, we numerically integrate equation 3, taking U as the complex field imposed by the pattern at the emission plane, and then find the OAM spectra using equation 4. We also experimentally measure the OAM spectrum using the method detailed below.

EXPERIMENTAL SET-UP

Figure 1 shows a schematic of our optical set-up. We use an SLM to encode the emitter phase pattern onto a planar wavefront of Gaussian intensity. The use of an SLM provides a flexible method to investigate a range of aperture configurations. A laser of wavelength 633 nm is

transmitted through a single mode fibre (to ensure we only have the TEM₀₀ mode present) and magnified to overfill SLM 1.

The emitter pattern is displayed on SLM 1, and consists of a ring of n regularly spaced circular apertures, each of radius r_a , as shown in Fig. 1(b). The radius of the ring is denoted by R . The maximum angular width subtended by each aperture is β radians, and as can be seen from the geometry of the pattern:

$$\beta = 2 \sin^{-1}(r_a/R). \quad (5)$$

The phase difference between adjacent apertures, $\delta\phi$, is set to advance in discrete steps. The size of $\delta\phi$ is controlled by the number of apertures, n , and an integer m defining the number of integer multiples of 2π the phase changes by around the entire ring. Therefore the phase difference between adjacent apertures is given by $\delta\phi = 2\pi m/n$, and the total phase change around the ring is given by $2\pi m$. Figures 1(d-k) show some examples of emitter phase patterns of varying n and m .

Within each aperture, a phase grating directs light (of the correct plane polarization, as each SLM only diffracts light of vertical polarization) into the first order of the resultant diffraction pattern. Light reflecting from the region around the apertures is directed to the zero order, where it is blocked by the spatial filter. The relative phase between each aperture is controlled by adjusting the phase of the vertical gratings. Adding a constant phase to all pixels within an individual aperture has the result of moving the positions of the ‘white-black’ phase wrapping lines sideways. Therefore the relative position of these lines from one aperture to the next defines the relative phase between apertures.

The field at SLM 1 is re-imaged to SLM 2 via a 4-f system, which enables the zero order undiffracted light from SLM 1 to be blocked, and any additional spatial filtering of the first order to be carried out if required. SLM 2 is used to measure the OAM spectrum of the resultant beam [24]. This is performed by sequentially displaying a series of phase gratings, defined by mode ℓ_{slm2} , on SLM 2, to test a series of OAM modes from $\ell_{slm2} = -20$ to $+20$. Each test mode ℓ_{slm2} adds an azimuthally varying phase $\ell_{slm2}\theta$ to the field. Incident light of mode $\ell = -\ell_{slm2}$ is transformed into a plane wave due to cancellation of the two phase terms of the same amplitude but opposite sign. Therefore light of this mode is focussed onto the optical axis of the first diffraction order by lens L_1 , and transmitted down another single mode fibre to a photodiode. Light of all other modes is not flattened to a plane wave but retains a non-zero orbital angular momentum, and is therefore not focussed onto the optical axis of the first diffraction order, and does not enter the single mode fibre to reach the photodiode. By cycling through values of ℓ_{slm2} in this manner, the signal at the photodiode records the intensity of light of each mode ℓ and the OAM spectrum is measured. We note that as

the OAM spectrum describes the relative power of each mode ℓ , the measurement hologram has no radial dependence. Therefore, each value of ℓ in the OAM spectrum represents a summation over all p accessible in our experiment, when considering the description of the fields in the LG basis set, as described earlier.

RESULTS

Measured OAM spectra. Figure 2 shows two measured OAM spectra for different emission pattern configurations. The spectra consist of a series of regularly spaced peaks multiplied by an envelope function. The data are comparable to a previous experiment, conducted by Yao et al. [25], who examined the OAM spectrum emitted from a set of ‘wedge’ shaped circular sector apertures. As described in [25], by considering the diffraction in cylindrical coordinates it can be shown that the separation of the peaks is given by the number of apertures, n , and the position of the fundamental peak (containing

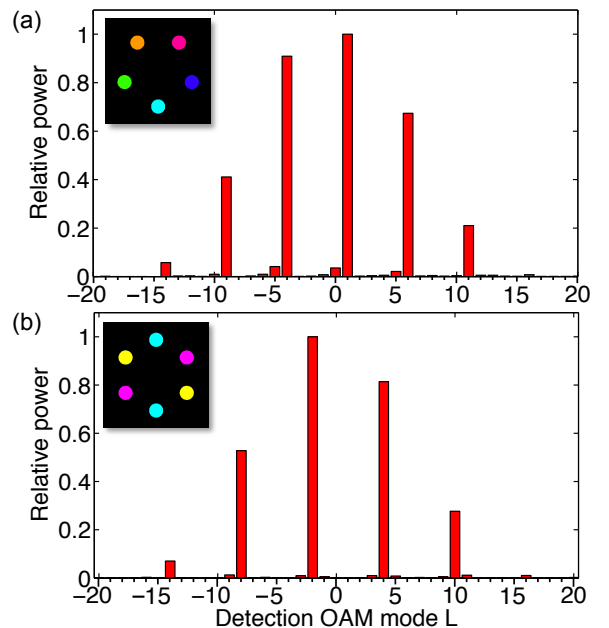


FIG. 2: Measured OAM spectra of light generated by a ring of circular apertures with phase patterns as shown in the top left of each spectra (phase scale is identical to that shown in Fig. 1). (a) 5 apertures, therefore the peaks in the OAM spectrum are separated by 5 modes. $m = 1$, i.e. a relative phase difference of $\delta\theta = 2\pi/5$ between neighbouring apertures, resulting in the maximum peak in the spectrum found at $\ell = 1$. (b) 6 apertures, $m = -2$, therefore $\delta\theta = \pi/3$ between adjacent apertures, resulting in a maximum peak in the spectrum found at $\ell = -2$. In each case the photodiode background signal (due to dark counts) has been subtracted from the measured signal, which has then been normalised by setting the dominant peak to a value of 1.

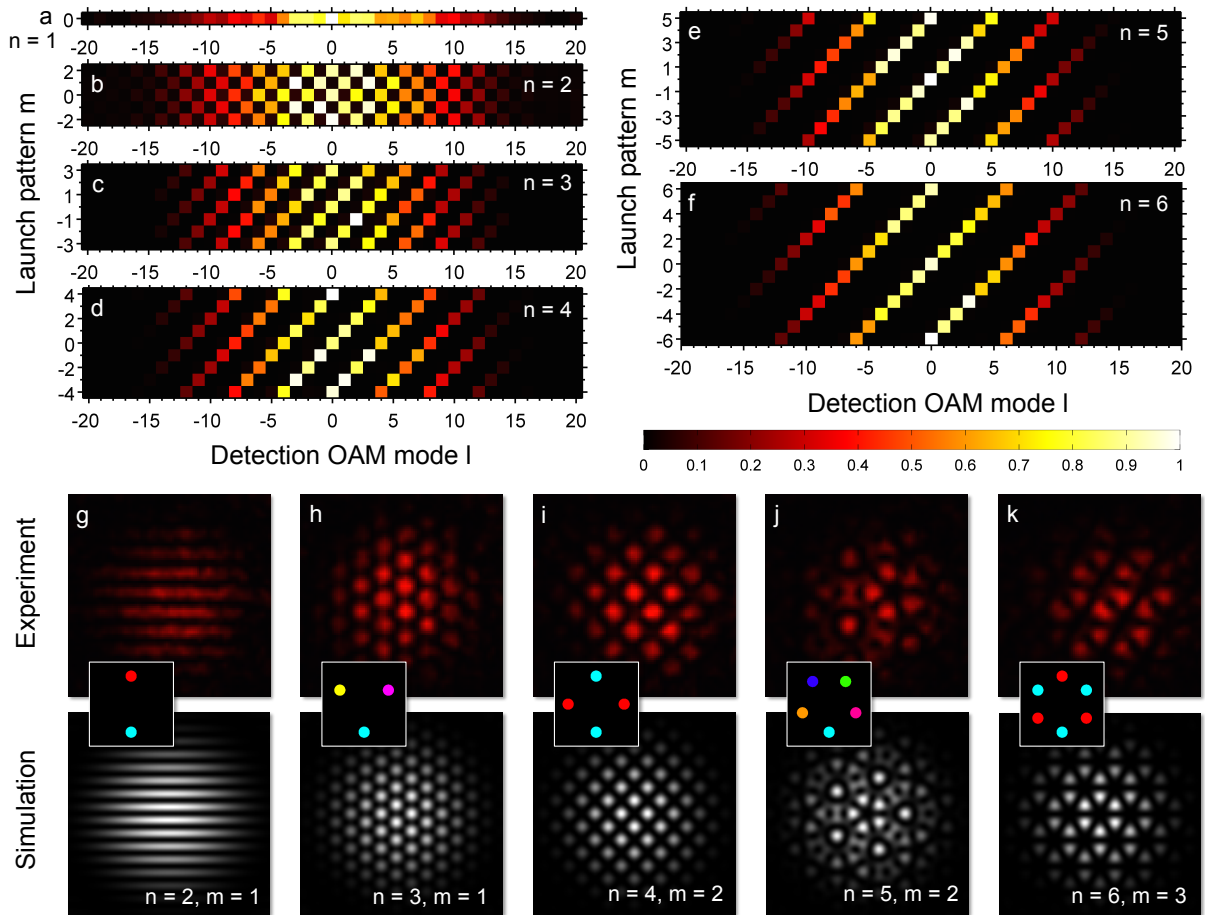


FIG. 3: (a) - (f) Variation in the measured OAM spectra with number of apertures n , and the integer multiple of 2π the phase changes by around the entire ring, m . Each row represents a single OAM spectrum of the type shown in Figure 2, with the relative height of the peaks captured by the colour of the intensity plot as given in the scale bar. The dominant value of the OAM spectrum can be controlled by appropriate selection of n and m . (g) - (k) show experimentally measured far-field diffraction patterns of selected emission patterns. The emission phase patterns are shown for each case. These are in good agreement with simulations of the system.

the most power) is given by $2\pi m$, the total phase difference around the pattern (for $|m| < n/2$). The shape of the spectra can be understood by analogy with the interference pattern generated by multiple linear slits [26]. Qualitatively the positioning of the peaks can be understood as the OAM values which have a high overlap with the emission pattern. For example, in 2(a), the phase at the centre of each aperture matches the phase at equivalent points in OAM beams of $\ell = 1, -4, 6, -9, 11$ etc., hence the presence of the peaks at these values.

Figures 3(a-f) show a series of OAM spectra for different numbers of circular emitters, n , and different values of m . The spectra are displayed as intensity plots, with each row representing the spectra of a particular choice of m (consider each row as looking down on bar graphs of the type shown in Fig. 2 from above, with the intensity indicating the height of the bar). Figure 3 shows that the relationship described in [25] also holds for the circular

aperture case. It can be seen that in each case the spectra have a fundamental peak at $\ell = m$, for $|m| < n/2$. Due to the periodicity of the peaks in the spectra, the dominant peak is always found within $\pm n/2$ of the origin. Analogously to the present case, the form of the spectra is also found in light transmitted from discretely stepped spiral phase plates, where the separation between peaks is given by the total number of steps [27].

Figures 3(g-k) show some examples of the far-field diffraction patterns of the emitted beam. Here we compare experimentally measured far-field patterns to simulated ones, and the agreement is evident. The simulation was performed by taking the 2D Fourier transform of the complex emission patterns, and here the intensity of the resulting field is displayed, as this is what is captured experimentally with a camera. The emission pattern is also shown for each case. We note that, as would be expected, these results are comparable to the far-field patterns cre-

ated by a beam carrying a defined OAM mode diffracted by a set of pinhole apertures, which can be used to identify the OAM mode in question [28].

The envelope function of the OAM spectra can be calculated by considering the Fourier transform of the transmission function of a single aperture, which follows by analogy with the case of linear diffraction from a single slit [26]. In the case of ‘wedge’ shaped apertures, the invariance of the angular spread of the aperture with radius simplifies the analysis, and results in an envelope function with a power proportional to $\text{sinc}^2(\alpha\ell/2)$, where α is the angular width of the wedge. This shape is a direct consequence of the angular uncertainty principle [29]: angular position and angular momentum are conjugate variables, and therefore subject to the Heisenberg uncertainty principle [29]. Therefore increasing α corresponds to an increased uncertainty in the angular position of photons that pass through the aperture, and therefore the uncertainty in their angular momentum is reduced, thus narrowing the OAM spectrum. In the present circular aperture case, despite the angular width of the circular apertures now being radially dependent, we find the difference in the envelope function from the ‘wedge’ case is small: the circular aperture envelope function is similar to that of a wedge aperture of angular width β , the maximum angular width subtended by the circular aperture (see Fig. 1(b)), as light from this radius will dominate the signal.

Figure 4 highlights how the efficiency with which the emission pattern produces OAM of a desired state (taken as that of the fundamental mode) is related to the angular uncertainty principle. We define the maximum efficiency as the fraction of power in the dominant OAM state, compared to the total transmitted power. As β is increased from an initial value, shown in Fig. 4(a), either by increasing r_a , shown in Fig. 4(d) or decreasing R , shown in Fig. 4(g) (as is evident from equation 5), the envelope function of the OAM spectra is narrowed. This reduces the amount of power in higher order (of the absolute value) modes and therefore increases the efficiency of power transmission into the dominant mode. This follows simply from the fact that the angular uncertainty of a photon in a beam of a pure single OAM state is 2π , i.e. the beam intensity profile is a full ring with no azimuthal variation in intensity for any specific radius.

Beam purification. We now show how the envelope function can be further modified by spatially filtering the beam emitted by SLM1. Low pass spatial filtering of the higher spatial frequencies of the discretely apertured emission plane (at SLM 1), is equivalent to performing a convolution of the complex field at the emission plane with an Airy function. This blurs both the intensity and phase information of the field at the emission plane into something that more readily approximates a beam carrying a single value of topological charge ℓ , as shown

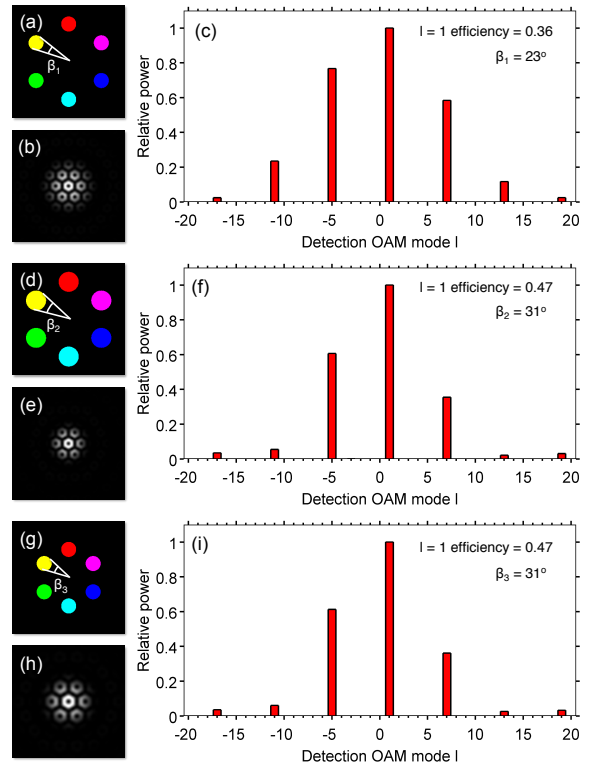


FIG. 4: Simulation demonstrating the relationship between β and transmitted efficiency. (a,d,g) emission patterns, (b,e,h) far-field intensity pattern and (c,f,i) OAM spectra.

in simulations in Fig. 5. This effect can also be understood by considering that spiral harmonics of increasing mode number $|\ell|$ form larger diameter rings at the Fourier plane (if considering a constant value of p). This means that higher (absolute) mode number spiral harmonics are formed from a linear sum of a set of higher spatial frequencies. Low pass spatial filtering removes these higher spatial frequencies, and therefore preferentially removes the higher (absolute) mode spiral harmonics, constricting the envelope function of the OAM spectrum. For this technique to work, the spectra must be odd, and therefore contain a single fundamental mode. In the case of even spectra, with two peaks symmetrically positioned about the origin, constricting the envelope function will purify both the positive and negative OAM modes to the same extent, and therefore not produce a beam of a *single* well defined OAM mode. The well separated peaks in the OAM spectra also facilitate this separation.

This process can also be understood qualitatively in terms of the angular uncertainty principle. In this case the uncertainty in angular momentum is reduced as the size of the spatial filter is decreased (by filtering out higher order modes with larger radii), and therefore the uncertainty in angular position is increased, transforming localised points of light that correspond to the apertures, into a continuous ring of light. Fig. 6 shows an experi-

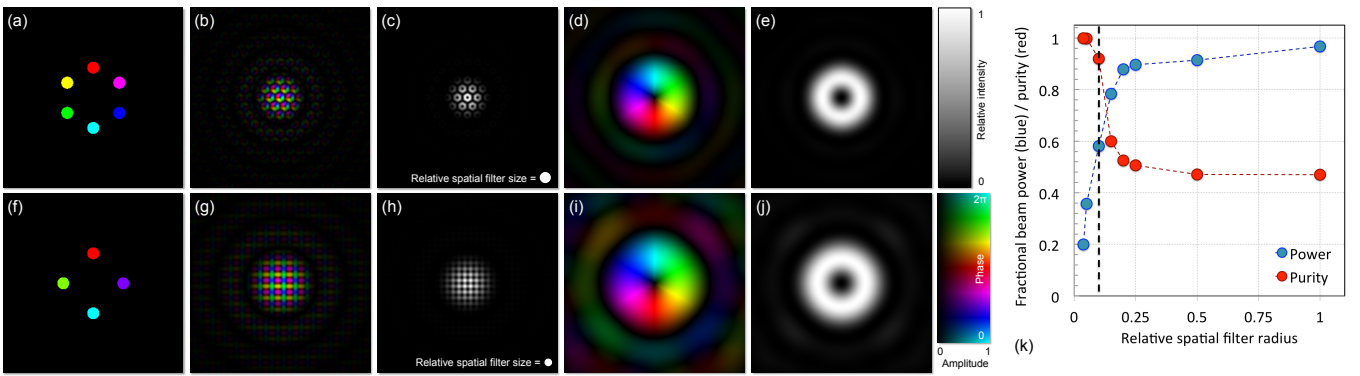


FIG. 5: Simulation showing the effect of spatially filtering the emitted beam. The case for two different emission patterns is shown. Top row: (a) $n = 6$, $m = 1$ emission pattern (equivalent to field at SLM 1). (b) far-field amplitude and phase, (c) far-field intensity, (d) Amplitude and phase of the conjugate image plane to (a) (equivalent to the field at SLM 2), after spatial filtering with the filter size shown in (c). It can be seen that a well defined mode is recovered. (e) Intensity of the conjugate image plane. Bottom row: (f-j) results for a emission pattern of $n = 4$, $m = 1$. (k) Simulated results showing the effect on the beam purity (red) and power in desired order (blue) as a fraction of the total power in the desired mode transmitted from the emission pattern shown in Fig. 4(g). For each point, the OAM spectrum of the beam was calculated by numerically integrating equations 1 to 4. As shown in Fig. 4(i), the initial efficiency (and therefore unfiltered purity of the dominant mode) is 0.47. As would be expected, when the unwanted modes are filtered out, some of the desired mode is also lost. In this example, to obtain a purity of 0.9, the power in the desired mode is reduced to 60% of its unfiltered value, as shown by the vertical hashed black line in (k).

mental demonstration of this effect. As the spatial filter diameter is reduced, the OAM spectrum is progressively constricted, and the image of the apertures recorded at the SLM 2 plane is further blurred, until it reaches the familiar doughnut shape of a beam carrying a well defined mode of OAM. In this case, the measured spectrum demonstrates a purity of 78%, calculated from the measured weight of the dominant peak in Fig. 6(d). The presence of the $\ell=2$ mode in Fig. 6(d) is most likely caused by a slight misalignment in the position of the spatial filter, causing a reduction in the measured purity of the beam [30].

Of course, by spatially filtering the beam in this way, unwanted light is removed and the total power in the output beam is reduced. Ultimately, the efficiency of OAM generation is related to how closely the complex emission profile matches that of the desired mode, and measurement of the OAM spectra of the emission plane is a direct quantification of this. Consequently, in the case considered here, emission patterns that exhibit a narrower OAM spectrum have a higher overlap integral with the desired fundamental mode. In Fig. 6(a), the beam purity of the $\ell=1$ mode is 24%, therefore this is the maximum efficiency with which we can expect to generate an $\ell=1$ beam. After spatial filtering to produce the beam shown in Fig. 6(d), 8% of the original transmitted power is found in the $\ell=1$, now with a purity of 78%. This reduction in the power of the desired mode is expected, as can be seen in Fig. 5(k), which shows how both the power in the desired mode, and the purity of the beam depend upon the size of the spatial filter. Ideally, the

relative size of the spatial filter can be tuned with respect to the size of the field in the Fourier plane, to maximise the transmitted efficiency. For example, in Figs. 4(e) and (h), β is held constant, but the scale of the far-field pattern is changed, therefore requiring a different sized spatial filter to purify the beam.

CONCLUSIONS

In this work we have investigated the OAM content of beams emitted from a ring configuration of discrete circular apertures of constant relative phase. We have shown that the OAM spectra of such an arrangement contains a comb of peaks, with a dominant peak at $\ell = m$, for $|m| < n/2$ where $2\pi m$ is the total variation in phase around a ring of n apertures. The condition $|m| < n/2$ arises from the fact that the dominant peak is always closest to the origin of the OAM spectrum and because the peaks are separated by n . We have shown how the envelope function of the spectra controls the maximum efficiency with which light is transmitted into the dominant mode. We have discussed how the envelope function, and therefore the efficiency of beam generation, is related to the angular uncertainty principle through the maximum angular width subtended by each aperture (β) in the emission pattern. We have also described how this envelope function can be further constricted by spatially filtering the beam, therefore suppressing the contributions of spiral harmonics of higher absolute values, and creating a beam of well-defined OAM.

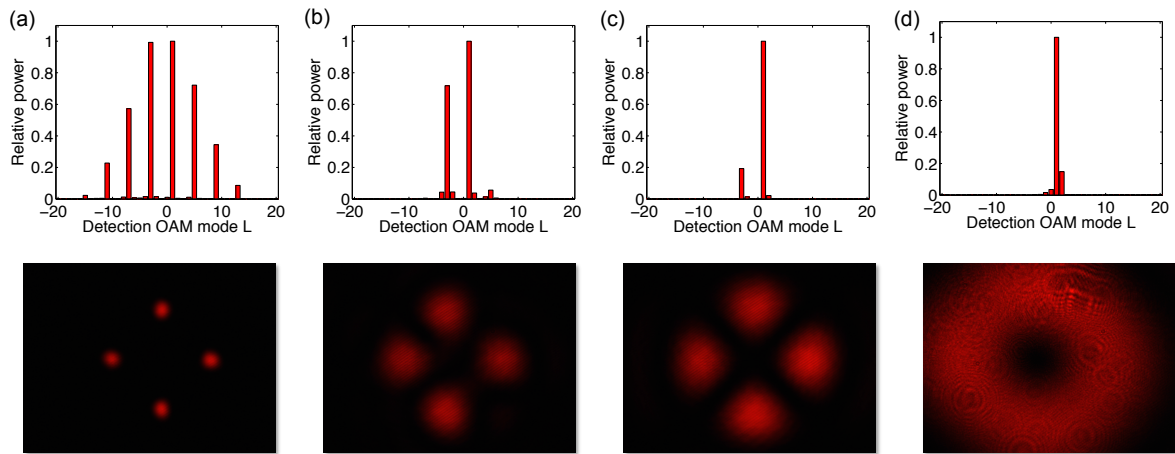


FIG. 6: Measured result of spatially filtering the emitted beam. The image below each graph shows the recorded intensity at SLM2. (a) OAM spectrum of the emitted beam with no spatial filtering. (b) to (d) OAM spectra and corresponding intensities at different levels of spatial filtering. (b) $400\mu\text{m}$ spatial filter. (c) $300\mu\text{m}$ spatial filter, (d) $150\mu\text{m}$ spatial filter. As the spatial filter size is reduced, the envelope function of the OAM spectra is further constricted. In (d) the characteristic ring shaped intensity distribution of a well-defined OAM mode is generated.

We note that the non-diffracting properties of light emitted from similar masks has also been investigated [31, 32]. The non-diffractive behaviour of beams emitted from such patterns can be seen from the fact that as n is increased, the emission profile approaches that of a ring slit aperture, which can be used to generate approximations to non-diffracting Bessel beams [33]. We also note that similar masks have been proposed to measure the OAM of an incident beam of a pure state of OAM [28].

More generally, finding simpler methods to generate beams of complex spatial modes creates beam shaping opportunities outside the optical regime where the equivalent to SLM technology does not currently exist [19, 20]. Our work highlights that the maximum efficiency with which light can be generated by a complex mask is given by the normalised overlap integral of the mask with the desired mode, and that it is also important to consider how efficiently the generated modes can be separated from one another.

ACKNOWLEDGEMENTS

This research was supported by the Engineering and Physical Sciences Research Council of the U.K. M.J.P. acknowledges support from the Royal Society. R.L. and F.L. were in part supported by the National Nature Science Foundation of China (Grant No. 11374239).

- [1] N. Simpson, K. Dholakia, L. Allen, and M. Padgett, *Optics Letters* **22**, 52 (1997).
- [2] V. L. Loke, T. Asavei, A. B. Stilgoe, T. A. Nieminen, and H. Rubinsztein-Dunlop, *Optics Express* **22**, 19692 (2014).
- [3] M. P. Lavery, F. C. Speirits, S. M. Barnett, and M. J. Padgett, *Science* **341**, 537 (2013).
- [4] D. Phillips, M. Lee, F. Speirits, S. Barnett, S. Simpson, M. Lavery, M. Padgett, and G. Gibson, *Physical Review A* **90**, 011801 (2014).
- [5] G. Gibson, J. Courtial, M. Padgett, M. Vasnetsov, V. Pas'ko, S. Barnett, and S. Franke-Arnold, *Optics Express* **12**, 5448 (2004).
- [6] M. Malik, M. OSullivan, B. Rodenburg, M. Mirhosseini, J. Leach, M. P. Lavery, M. J. Padgett, and R. W. Boyd, *Optics express* **20**, 13195 (2012).
- [7] J. Wang, J.-Y. Yang, I. M. Fazal, N. Ahmed, Y. Yan, H. Huang, Y. Ren, Y. Yue, S. Dolinar, M. Tur, et al., *Nature Photonics* **6**, 488 (2012).
- [8] L. Allen, M. Beijersbergen, R. Spreeuw, J. Woerdman, et al., *Physical Review A* **45**, 8185 (1992).
- [9] N. Heckenberg, R. McDuff, C. Smith, and A. White, *Opt. Lett* **17**, 221 (1992).
- [10] N. Heckenberg, R. McDuff, C. Smith, H. Rubinsztein-Dunlop, and M. Wegener, *Optical and Quantum Electronics* **24**, S951 (1992).
- [11] J. Arlt, K. Dholakia, L. Allen, and M. Padgett, *Journal of Modern Optics* **45**, 1231 (1998).
- [12] R. W. Bowman, G. M. Gibson, A. Linnenberger, D. B. Phillips, J. A. Grieve, D. M. Carberry, S. Serati, M. J. Miles, and M. J. Padgett, *Computer Physics Communications* **185**, 268 (2014).
- [13] X. Cai, J. Wang, M. J. Strain, B. Johnson-Morris, J. Zhu, M. Sorel, J. L. O'Brien, M. G. Thompson, and S. Yu, *Science* **338**, 363 (2012).
- [14] M. J. Strain, X. Cai, J. Wang, J. Zhu, D. B. Phillips,

- L. Chen, M. Lopez-Garcia, J. L. OBrien, M. G. Thompson, M. Sorel, et al., *Nature communications* **5** (2014).
- [15] M. M. Coles, M. D. Williams, K. Saadi, D. S. Bradshaw, and D. L. Andrews, *Laser & Photonics Reviews* **7**, 1088 (2013).
- [16] M. D. Williams, M. M. Coles, D. S. Bradshaw, and D. L. Andrews, *Physical Review A* **89**, 033837 (2014).
- [17] B. T. Hefner and P. L. Marston, *The Journal of the Acoustical Society of America* **106**, 3313 (1999).
- [18] J. Verbeeck, H. Tian, and P. Schattschneider, *Nature* **467**, 301 (2010).
- [19] R. Dall, M. D. Fraser, A. S. Desyatnikov, G. Li, S. Brodbeck, M. Kamp, C. Schneider, S. Höfling, and E. A. Ostrovskaya, *Physical review letters* **113**, 200404 (2014).
- [20] Z. Li, M. Zhang, G. Liang, X. Li, X. Chen, and C. Cheng, *Optics express* **21**, 15755 (2013).
- [21] J. Sun, X. Wang, T. Xu, Z. A. Kudyshev, A. N. Cartwright, and N. M. Litchinitser, *Nano letters* **14**, 2726 (2014).
- [22] C. Schulze, S. Ngcobo, M. Duparré, and A. Forbes, *Optics express* **20**, 27866 (2012).
- [23] C. Schulze, A. Dudley, D. Flamm, M. Duparré, and A. Forbes, *New Journal of Physics* **15**, 073025 (2013).
- [24] J. Leach, M. J. Padgett, S. M. Barnett, S. Franke-Arnold, and J. Courtial, *Physical review letters* **88**, 257901 (2002).
- [25] E. Yao, S. Franke-Arnold, J. Courtial, S. Barnett, and M. Padgett, *Optics express* **14**, 9071 (2006).
- [26] B. Jack, M. Padgett, and S. Franke-Arnold, *New Journal of Physics* **10**, 103013 (2008).
- [27] C.-S. Guo, D.-M. Xue, Y.-J. Han, and J. Ding, *Optics communications* **268**, 235 (2006).
- [28] G. C. G. Berkhout and M. W. Beijersbergen, *Physical Review Letters* **101**, 100801 (2008).
- [29] S. Franke-Arnold, S. M. Barnett, E. Yao, J. Leach, J. Courtial, and M. Padgett, *New Journal of Physics* **6**, 103 (2004).
- [30] M. Vasnetsov, V. Pas'ko, and M. Soskin, *New Journal of Physics* **7**, 46 (2005).
- [31] Z. Bouchal, *Czechoslovak journal of physics* **53**, 537 (2003).
- [32] M. Boguslawski, P. Rose, and C. Denz, *Physical Review A* **84**, 013832 (2011).
- [33] R. Vasilyeu, A. Dudley, N. Khilo, and A. Forbes, *Optics express* **17**, 23389 (2009).